Roles of PknB and CslA in cell wall morphogenesis of *Streptomyces*

Marta Derkacz[1], Andrew Watson[2], Akshada Gajbhiye[3], Dagmara Jakimowicz[1], Matthias Trost[3] Jeff Errington[2,4] and Bernhard Kepplinger[1,2*]

[1] University of Wroclaw, Department of Molecular Microbiology, ul. F. Joliot-Curie 14a, 50-383 Wrocław, PL

[2] Newcastle University, Centre for Bacterial Cell Biology, Baddiley-Clark Building, Newcastle upon Tyne NE2 4AX, UK

[3] Newcastle University Biosciences Institute, Faculty of Medical Sciences, Newcastle upon Tyne, NE2 4HH, UK

[4] The University of Sydney, Faculty of Medicine and Health, Sydney, NSW 2006, AU

* Corresponding author: bernhard.kepplinger@uwr.edu.pl

Key words: PknB, CslA, RodA, Tip Organising Centre (TIPOC), polarisome, cell morphogenesis, cell wall, phosphorylation, *Streptomyces*

Abstract

Streptomyces are filamentous bacteria living mostly in the soil and best known for their ability to produce specialised metabolites, including antibiotics. They grow as tip-extending, branching hyphal filaments to form a multicellular mycelium. New branches are established by the formation of a new growth zone on the lateral cell wall. Proteins responsible for this process are organised in complexes called polarisomes, with DivIVA being the best described component. We have developed a genetic screen based on DivIVA overexpression to identify proteins potentially interacting with DivIVA in *Streptomyces albus*. Among the hits was the morphology controlling protein *rodA* and the kinase *pknB*.

We confirmed that deletion of *pknB* rescues *S. albus* from the effects of overexpressing DivIVA. Next, we studied the impact of *pknB* deletion in *Streptomyces.* A mass spectrometry phosphoproteome analysis indicated that absence of PknB alters the phosphorylation state of CslA, a cellulose synthase-like protein, containing a glycosyltransferase domain. We demonstrate that a phosphoablative mutant of CslA impacts its activity in β-glucan synthesis, as displayed by a hypersensitivity to lysozyme. Our findings highlight the role of PknB in maintaining the cellular structure and integrity of the *Streptomyces* cell wall.

Importance

A thorough understanding of the regulatory mechanisms of cell wall biosynthesis and integrity in *Streptomyces* is fundamentally important, as these are linked to antibiotic production. This study investigates the role of the kinase PknB, which we identified via a genetic screen. Through a phosphoproteome analysis, we identified that PknB regulates the activity of CslA, a protein crucial for β-glucan synthesis. By demonstrating the impact of PknB, this research provides novel insights into the molecular pathways influencing *Streptomyces* resilience. This research not only enhances our understanding of cell morphogenesis but also has potential implications for developing new strategies to optimize antibiotic production.

Introduction

The maintenance of bacterial cell wall integrity is crucial for its survival, as the cell would otherwise succumb to lysis caused by osmotic shock. Beyond differences in cell wall structure (e.g. Gram-positive vs. Gram-negative) or general morphological features (coccoid vs. rod), bacteria can be categorized based on the location of peptidoglycan insertion. Peptidoglycan is an essential component of bacterial cell walls, providing structural integrity and rigidity, which enables bacteria to maintain their shape and withstand osmotic pressure. The bacteria arguably best studied for cell morphogenesis are *Proteobacteria* (e.g. *Escherichia coli*) and *Firmicutes* (e.g. *Bacillus subtilis*). A shared characteristic among these rod-shaped bacteria is the lateral insertion of cell wall material, while the poles remain inert. In stark contrast, some bacteria including *Actinobacteria* (e.g. *Streptomyces or Mycobacteria*) insert new cell wall material only at the tip. These can be further divided into unicellular bacteria such as *Mycobacteria* or *Corynebacteria* or into multicellular bacteria like *Streptomyces*. In *Streptomyces*, apart from tip growth, new growth zones are created laterally by the formation of branches, ultimately leading to a complicated mycelium. Proteins of cell wall biosynthetic machinery, responsible for tip growth, are locally organised in complexes called TIP Organising Centres (TIPOCs) or polarisomes (1). Within the polarisome, a pivotal protein is DivIVA, a coiled-coil protein that is indispensable in *Streptomyces* (2). It plays a crucial role by localizing to cell growth sites and directing localised cell wall synthesis. New DivIVA complexes appear on the lateral wall in parallel with the formation of new branch sites (1–3). While the precise mechanism behind the establishment of new branches remains unclear, they tend to occur preferentially at curved segments of the cell wall (1).

Two additional scaffolding proteins Scy and FilP are believed to sequester DivIVA, facilitating the establishment of new growth zones and influencing the size and positioning of DivIVA complexes, respectively (4, 5). An overproduction of DivIVA causes swollen tips and hyperbranching most likely due to misregulation of the cell wall biosynthetic machinery (2).

DivIVA phosphorylation has been reported in a wide range of species (6–8). While *Streptomyces coelicolor* encodes at least 34 Ser/Thr kinases, DivIVA was shown to be modified by the non-essential Ser/Thr kinase AfsK (9). The recently identified phosphatase SppA seems to serve as the counterpart in that process (10). Importantly, overexpression of AfsK causes disassembly of the apical (mother) polarisome, leading to the creation of multiple daughter polarisomes, which is followed by the establishment of multiple hyphal branches (1). The AfsK phosphorylation sites in

DivIVA were identified by mass spectrometry as occurring on the non-essential C-term domain of the protein, at residues T304, S309, S338, S344, and S355 (11).

In *Mycobacteria* the DivIVA homologue Wag31, is phosphorylated by the essential kinases PknA and PknB (12). Interestingly a knockout of the homologous kinase PknB in *Streptomyces* has no detrimental effect, while the kinase PknA is missing in most *Streptomyces spp.* (13).

Another important target of PknB, in *Mycobacteria* is RodA in *Mycobacteria*, is a highly conserved member of the SEDS (Shape, Elongation, Division, and Sporulation) family of proteins (14, 15). It possesses glycosyltransferase (GTase) activity, which is crucial for the synthesis of glycan strands. These strands, along with cross-links generated by transpeptidases (TPase), together form peptidoglycan (16). In contrast to other mycobacterial systems, RodA is essential in *Streptomyces* (17).

In this study, we aimed to deepen our understanding of the polarisome complex and its adaptation, as well as the intricate regulation of cell morphogenesis in *Streptomyces*. To achieve this, we developed a suppressor screen to identify the connections between proteins involved in the complex regulation of cell morphogenesis.

Materials and methods

Bacterial strains and culture conditions

All *S. albus* strains used in this study are listed in Tab. S1. *S. albus* spores were collected using standard protocols (18) from cultures grown on Soya Flour Mannitol (SFM) agar plates supplemented with antibiotics (if required) to a final concentration of: apramycin (50 ng/mL) and hygromycin (50 ng/mL). Spore concentration was determined using a serial dilution on SFM agar plates. Spores were maintained at -80 ºC, in 25% glycerol aliquots for one use. For morphology experiments Tryptic Soy Broth (TSB) and 5% TSB were used. Liquid cultures were performed in 250 mL Erlenmeyer flasks containing metal spirals (30 ºC, 220 rpm). Solid cultures were grown on 20 mL of TSA (TSB, 2% agar) or 5% TSA (5% TSB, 2% agar) plates at 30 ºC. *E. coli* strains (listed in Tab. S2) were grown at 37 ºC on LB supplemented with antibiotics (if required) to a final concentration of: apramycin (50 ng/mL), kanamycin (50 ng/mL), chloramphenicol (34 ng/mL) or on 2YT supplemented with hygromycin (50 ng/mL).

Construction of plasmids and strains

All plasmids and oligonucleotides used in this study are listed in Tab. S3 and Tab. S4, respectively. For details of plasmids construction see SI. Plasmids were transformed to *E. coli* DH5α strain and then transferred to *Streptomyces* by conjugation with *E. coli* ET12567/pUZ8002 strain or protoplast transformation, using standard protocols (18).

Selection of spontaneous suppressor mutants and bioinformatic analysis

Spores of the DivIVA overproduction strain (approximately 10^6 spores per plate) were spread onto 5% TSA plates with 500 ng/mL of inducer (anhydrotetracycline). After 5 days, several colonies could be observed, and these were restreaked on fresh 5% TSA containing 500 ng/mL of inducer (anhydrotetracycline). The parent DivIVA overproduction strain and the wild type were used as controls.

DNA was isolated from strains using a modified version of the "salting-out" method (19, 20). Libraries for Illumina sequencing were prepared using the Illumina DNA prep kit with Nextera XT kit and the Illumina Nextera XT primer Index Kit. Libraries were sequenced by Edinburgh genomics on an MiSeq v2 250PE. Raw sequences are available in NCBI Sequence Read Archive (accession number PRJNA1099611).

The quality of all Illumina reads was checked using fastQC (version 0.11.9), and reads were trimmed using trimmomatic (version 0.39). Trimmed Illumina reads were aligned to the

Streptomyces albus J1074 genome (NC_020990.1) using bowtie2 (version 2.3.5.1) and the very-sensitive preset mode for mapping paired end reads. Variants were called using the bcftools (version 1.14) in the consensus calling mode (-c). Only predicted variants with a QUAL score of >=15 were retained. Bedtools subtract (version 2.27.1) was used to filter out any variants identified in potential suppressor strains that were already present in the lab *S. albus* J1074 parent strain compared to the reference sequence (NC_020990.1), and thus were accumulated independently from this experiment. The potential impact of all variants on protein-coding sequences was assessed using snpEff (version 5.0e) (21).

Microscopy

For phenotype analysis, 10^7 CFU (colony forming units) of *S. albus* J1074 strains were inoculated in 20 ml TSB or 5% TSB in the presence or absence of ATc (anhydrotetracycline) (250 ng/mL) and cultured for 20 hours.

For β-glucans staining, $2 \cdot 10^6$ CFU (estimated by OD_{600} measurement) of *S. albus* J1074 strains, from freshly grown SFM agar plates, were inoculated in 20 ml TSB and cultured for 20 h. Cells were centrifuged and washed with modified PEM buffer (0.4 M PIPES, 20 mM EDTA, 20 mM $MgCl_2$; pH = 6.9 (KOH)), stained with Lectin dye (Sigma-Aldrich L3892) for 5 min at room temperature, washed and resuspended with modified PEM buffer (22).

Cells were centrifuged if needed, loaded on 1,2% agarose slide before imaging and examined by Leica DM6 B fluorescence microscope equipped with a 100× objective with a DFC7000 GT camera. Pictures were analysed using ImageJ software.

For determination of β-glucans content (Fig. 4), a mean fluorescence signal was measured at each tip (within the circle with a diameter of 20 pixels). Minimum data points collected for each strain were 574. (22) Data were analysed and visualised using R software, including the ggplot2 package (23). Statistical analysis was performed using ANOVA followed by Tukey's HSD post-hoc test.

Mass Spectrometry

For mass spectrometry, 10^7 CFU of WT or Δ*pknB* were inoculated in 50 mL of TSB or 5% TSB and cultured for 20 hours. Four biological repeats were performed for each condition. Mycelia were harvested by centrifugation (5 min, 4 ºC, 3000 x g), washed twice with PBS and resuspended in 8 M urea buffer supplemented with 50 mM Tris, 1 mM TCEP (Roth), protease inhibitor (Thermo Scientific) and phosphatase inhibitor (sodium molybdate 115 mM, sodium orthovanadate 100 mM, sodium tartrate dihydrate 400 FigmM, glycerophosphate 500 mM, sodium fluoride 100 mM). 5

mL of buffer were used for each 1 g of biomass. Cells were disrupted by sonication (2 x 20 s, 4 ºC, 20 kHz), centrifuged (15 min, 4 ºC, 3000 x g) and supernatant was kept in -80 ºC before next steps. Detailed protocol of samples preparation and mass spectrometry analysis is available in SI.

Lysozyme and antibiotics sensitivity and survival assays

Sensitivity to lysozyme and antibiotics were tested by inoculating 5 µl of PBS spore suspension, containing 10^4, 10^3, 10^2, 10 and 1 CFU, on TSA and 5% TSA supplemented with antibiotics or lysozyme and compared to a no addition control (concentrations shown in Fig. 2, 3, S4 and S7). Survival assays were performed similarly, using TSA and 5% TSA, both supplemented or not with anhydrotetracycline 500 ng/mL. Addition of 0.5 M of sucrose to 5% TSA was tested to determine the impact of osmotic stress conditions of 5% TSA on inducible DivIVA production strain (called 65α) lethality.

DivIVA-mScarlet production analysis

For western blot analysis, 2 x 10^7 CFU of *Streptomyces* strains were inoculated in 50 mL of TSB or 5% TSB, in the presence or absence of ATc (250 ng/mL) and cultured for 24 hours. Up to 50 mL of cultured mycelia were harvested by centrifugation (5 min, 4 ºC, 3000 x g), washed twice with PBS and resuspended in 1 mL PBS supplemented with protease inhibitor (Thermo Scientific) and 1 mM DTT. Cells were disrupted by sonication (2 x 20 s, 4 ºC, 20 kHz), mixed with 6xLB and denatured (15 min, 95 ºC). Total protein concentration was normalized and assessed on an SDS-PAGE containing 2,5% 2,2,2-Trichloroethanol (Thermo Scientific) and the proteins were visualised by stain free filter on a ChemiDoc (BioRad). The signal intensity was measured in ImageJ and the samples were adjusted accordingly (for loading gel control see Fig. S1). Proteins were transferred to a nitrocellulose membrane, which was blocked with blocking solution (5% powder milk in PBST (PBS with 0.1% Tween-20)), then incubated with rabbit anti-mCherry polyclonal purified antibody (Invitrogen, diluted 1:1000 in fresh blocking solution). Membrane was washed three times with PBST and incubated with goat anti-rabbit IgG cross-linked to horseradish peroxidase (Santa Cruz Biotechnology, diluted 1:5000 in fresh blocking solution), then washed three times with PBST. Blot was incubated with SuperSignal™ West Pico PLUS Chemiluminescence Substrate (ThermoScientific) and visualised by ChemiDoc (BioRad).

Results and Discussion

Identification of conditions for lethality of a DivIVA overexpression construct

The scaffolding protein DivIVA is localised at the tip of the hyphae and is essential for the apical extension of the cell wall (1, 2). It was shown that overproduction of DivVIA leads to swelling of the tip, most likely by misaligning the cell wall biosynthetic machinery (1).

In an attempt to discover previously unknown interactions crucial for the polarisome complex, we hypothesized that a suppressor mutation capable of rescuing cells from lethal DivIVA overproduction might be in a gene encoding for a protein that interact, directly or indirectly, with DivIVA or other components of the polarisome complex.

Initially, we endeavoured to induce lethality in a strain carrying an additional copy of *divIVA* gene under the control of inducible promoter, located in the BT1 locus, and encoding for DivIVA-mScarlet fusion. We experimented with various conditions such as different media and temperatures, but without success. Consequently, we opted to modify the promoter of the native copy of the *divIVA* gene as well. This led to the creation of a strain, designated 65α, harbouring two inducible copies of *divIVA-mScarlet* - one in the native locus and the other in the BT1 locus (Fig. 1A). Surprisingly, although a divIVA null mutation is lethal (2) this strain was able to grow in the absence of the inducer, presumably because of leaky expression from the tetracycline-inducible promoter. However, upon induction, a strong fluorescence signal was observed at hyphal tips, accompanied by swelling and hyperbranching (Fig. 1C), aligning with previously documented observations from a DivIVA overproduction strain of *S. coelicolor* (1, 2). After testing a range of growth conditions, we found that under hypoosmotic-stress conditions (1/20 reduced concentration of TSA medium “5% TSA”), growth of strain 65a was abolished in the presence of the inducer, while it grew similarly to the wild type in its absence (Fig. 1B). The growth inhibition was probably due to cell wall damage, leading to osmotic lysis, as growth was rescuable by the addition of 0.5 M sucrose (Fig. S2).

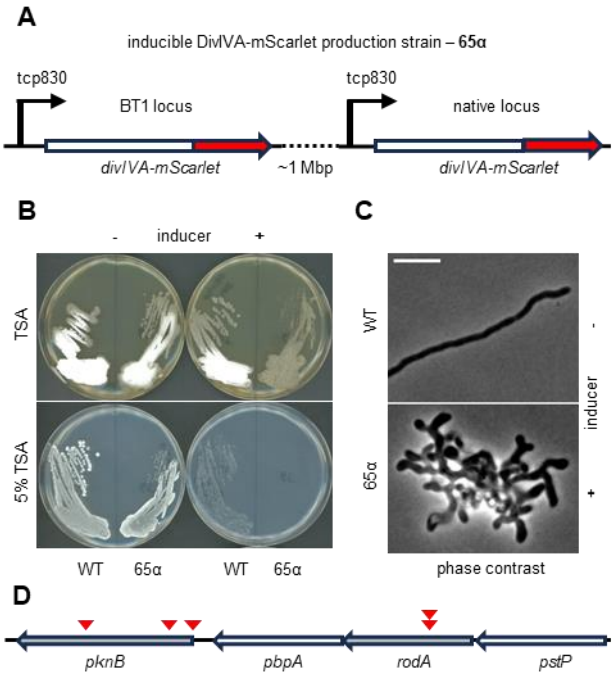

Figure 1 Genetic configuration and phenotypic analysis of *S. albus* J1074 mutant strain 65α with inducible *divIVA-mScarlet* fusion (A) Pictorial representation of the genetic makeup of the *S. albus* J1074 mutant, called 65α, containing two copies of a *divIVA-mScarlet* fusion under the control of the anhydrotetracycline (ATc) inducible promoter tcp830. (B) Comparison of the growth behaviour of the wild type *S. albus* J1074 and the inducible mutant strain 65α on TSA and 5% TSA in the presence or absence of the inducer. (C) Microscopical phenotype of the *S. albus* J1074 wild type strain and 65α mutant grown in TSB. Scale bar - 5 µm. (D) Genetic organization of the gene cluster containing *pknB* and *rodA* in *S. albus* J1074 (3,450,591-3,457,165 on NC_020990; ~1Mbp from BT1 locus and ~2Mbp from *divIVA* locus). Red arrows indicate the localisation of the mutations stated in detail in Table 1.

Table 1 Proteins encoded by genes identified in more than one mutant arising from the suppressor screen. Number of mutants refers to how often a mutation in the gene was recovered in a different mutant strain. Amino acid change indicates the result of a mutation in the corresponding mutant strain starting with M. Note that some mutants have more than one mutation in the same gene. fs – frame shift; del – deletion; ins – insertion, * – stop codon.

GENE	ANNOTATION	MUTANT NUMBER	AMINO ACID CHANGE
XNR_RS00945	hypothetical protein	2	M43:P57R; M43:P57S; M25:A77A
XNR_RS06115	CAP domain-containing protein	2	M26:Q195fs; M37:Q195fs
XNR_RS06760	potassium-transporting ATPase subunit KdpB	2	M29: S23G; M25: S23fs
XNR_RS08380	prolyl oligopeptidase family serine peptidase	2	M43:P63fs; M34:P63fs
XNR_RS12415	cobalamin-dependent protein	2	M26: A88V; M26: A87A; M19: D202A
XNR_RS12645	DUF3631 domain-containing protein	2	M29: N385fs; M37: N385fs
XNR_RS13425	TadE family type IV pilus minor pilin	2	M37: G39R; M37: A38A; M19: G39G; M19: G39A; M19: G39R; M19: A38A
XNR_RS14820	MFS transporter	2	M29: R301P; M29: R302S; M29: G304R; M33: R301P

XNR_RS15060	Stk1 family PASTA domain-containing Ser/Thr kinase	3	M43: S98fs; M40: A396D; M25: M1fs
XNR_RS15070	FtsW/RodA/SpoVE family cell cycle protein	2	M34: L162del; M33: L162del
XNR_RS15980	alanine--tRNA ligase	3	M3: G863_G864insV; M40: G863_G864insV; M33: G863_G864insV
XNR_RS17095	non-ribosomal peptide synthetase	2	M7: A3035fs; M3: A3035fs
XNR_RS23500	C40 family peptidase	2	M29: M315I; M33: H288fs
XNR_RS28225	FAD-dependent oxidoreductase	5	M30: R327P; M40: R327P; M40: R326R; M40: R326C; M40:R325R; M40: W324*; M37: R326R; M37: R325R; M33: W324*; M20: R326R; M20: R326C; M20: R325R; M20: R324*

A suppressor screen for mutations bypassing DivIVA overexpression lethality

To identify genes encoding proteins potentially interacting with DivIVA, we plated strain 65a under the lethal conditions described above and picked colonies that emerged, which we expected would contain spontaneous mutations suppressing the lethal phenotype. In total we picked 43 mutants of three different cultures, of which 13 displayed robust growth under, for 65α, lethal conditions.

Because we had two separate copies of the *divIVA* construct, we expected the new mutations to lie in genes other than *divIVA* itself. We therefore carried out whole genome sequencing using Illumina technology. Bioinformatic analysis of the sequences of the 13 mutants revealed apparent mutations in 122 coding regions. We compared the mutations and found several that occurred in multiple mutant strains, suggesting that they might be clonal mutations (Table 1, for the full list see File S1).

Of the genes identified, XNR_RS15060 and XNR_RS15070 stood out as particularly interesting. These genes are located almost adjacent to each other, and their identities are apparent by conservation of the gene cluster relative to other actinobacteria. They were annotated as *pknB* (XNR_RS15060) and *rodA* (XNR_RS15070) (Fig. 1D). Moreover, both genes encode proteins involved in cell envelope maintenance. While *pknB* had three unique mutations, *rodA* contained the same mutation in mutant strains recovered from the same plate which could indicate a clonal relationship. The kinase PknB is an essential protein in *Mycobacterium tuberculosis* (24) and *Corynebacterium glutamicum* (25). *pknB* mutations affect the maintenance of cell shape, while the glycosyltransferase (GTase) RodA is one of its phosphorylation targets (14, 26). PknB also phosphorylates DivIVA in *Mycobacteria*, though not in *Streptomyces* (8, 9). RodA is also known

to interact with DivIVA in *Corynebacterium glutamicum* (27). The exact role of PknB in *Streptomyces* has not been elucidated, as deletion of *pknB*, in contrast to other bacteria, has no deleterious effect, at least in otherwise wild type cells (13). The network of interactions described above, involving various proteins involved in cell morphogenesis prompted us to focus on the role of PknB.

Deletion of *pknB* rescues *Streptomyces* from lethal overexpression of DivIVA

To test whether the mutations identified above were responsible for suppression of the *divIVA* overexpression phenotype we attempted to delete *pknB* in wild type and 65α strains.

It was previously shown in *S. coelicolor* that it was possible to delete RodA only when another copy of the gene was integrated at the φ31 *att* site, indicating its essentiality (17). In preliminary studies we also tried but failed to delete the gene using the CRISPR/Cas9 technology indicating that *rodA* is also essential in *S. albus*.

In contrast, deletion of *pknB* had no evident phenotype in the wild type *S. albus* strain, again consistent with previously reported data (13). However, in the 65α background the deletion of *pknB* allowed the strain to grow under otherwise lethal conditions (5% TSA in the presence of the inducer of *divIVA-mScarlet*) (Fig. 2A).

To study how the Δ*pknB* mutation rescued the effects of *divIVA-mScarlet* overproduction we used various microscopic imaging methods to compare the morphological phenotype of the 65α Δ*pknB* strain to those of both its parent strain 65α and the wild type (Fig. 2B). The 65α strain showed an increased frequency of branching compared with the wild type, even in the absence of the inducer, and in the presence of ATc, it exhibited hyperbranching, bulging and an accumulation of mScarlet at the hyphal tips. In contrast, the 65α Δ*pknB* strain had reduced branching and a diminished fluorescent signal compared with 65α. Indeed 65α Δ*pknB* mycelia closely resembled those of the wild type strain, even in the presence of ATc. Although we could still detect a fluorescent signal from mScarlet, it was notably weaker than in the case of 65α. We conducted Sanger sequencing of the fusion gene *divIVA-mScarlet* in both loci and found that neither contained a mutation. Presumably, the lowered signal at hyphal tips could be a result of DivIVA-mScarlet being distributed more widely throughout the hyphae, or to diminished protein levels through decreased synthesis or increased degradation. To investigate this, we directly compared DivIVA-mScarlet levels in 65α and 65α Δ*pknB* by Western blotting using a purified antibody against mScarlet (Fig.

2C). We observed a reduced signal of the mScarlet when comparing 65α to 65α Δ*pknB*, consistent with the microscopy data. However, in 65α Δ*pknB*, in addition to the full-length DivIVA-mScarlet (68 kDa but apparently migrating more slowly, close to the 100 kDa marker, possibly due to the formation of a dimer), multiple faster migrating peptides were detected. These peptides are presumably cleavage products containing all or part of mScarlet (26.4kDa). Thus, lowered levels of DivIVA-mScarlet in absence of PknB are most likely responsible for rescuing the growth of the 65α mutant.

PknB phosphorylates RodA, which alters the sensitivity to moenomycin

Given the role of DivIVA in cell wall synthesis we expected that the 65α strain had an altered cell wall structure, making it more susceptible to osmotic fluctuations. We tested this by addition of an osmoprotectant (0.5 M sucrose) to the otherwise lethal condition of 5% TSA. This allowed the strain to proliferate once again, which supported the idea that an altered cell wall structure was responsible for lethality of strain 65α on 5% TSA in the presence of inducer (Fig. S2). If so, a *pknB* deletion mutant might also be more susceptible to cell-wall-targeting antibiotics. We, therefore, tested the relative sensitivity of a *pknB* single mutant in the wild-type background to various cell wall antibiotics: carbenicillin, vancomycin, bacitracin, moenomycin (for scheme see Fig. S3), including chloramphenicol (targeting protein synthesis) as a control. The *pknB* deletion mutant exhibited increased sensitivity to all but one of the cell wall-targeting compounds compared to the wild type control (Fig. S4). Surprisingly, however, the *pknB* mutant was hyper-resistant to the antibiotic moenomycin (Fig. 2D). Moenomycin acts on the GTase activity specifically of class A PBPs, while the RodA GTase is unaffected (28).The absence of PknB can result in hyper-resistance to moenomycin due to the increased activity of RodA. Under normal conditions, PknB might play a critical role in regulating RodA's activity. However, in the absence of PknB, RodA becomes overactive, leading to enhanced transglycosylation and therefore increased resistance to moenomycin. PknB from *M. tuberculosis* was previously shown to phosphorylate a C-terminal fragment of RodA in an *E. coli* in vitro system (14). Furthermore, in *Streptomyces rimosus*, the equivalent residue to that phosphorylated in the in vitro system (T469) was reported to be phosphorylated in vivo (29) (for alignment see Fig. S6). We speculated that this residue is responsible for an altered activity of RodA. To test the possible role of T469 phosphorylation on RodA function in *S. albus* we constructed a phosphoablative mutation (*rodA*$_{(T469A)}$) using

CRISPR/Cas9 technology. This strain exhibited increased resistance to moenomycin compared to the wild type, indicating that T469 is indeed important for RodA function, although, the level of resistance was not as great as for the deletion of *pknB* (Fig. 2D). Nevertheless, the results suggest that phosphorylation by PknB is important for the GTase activity of RodA.

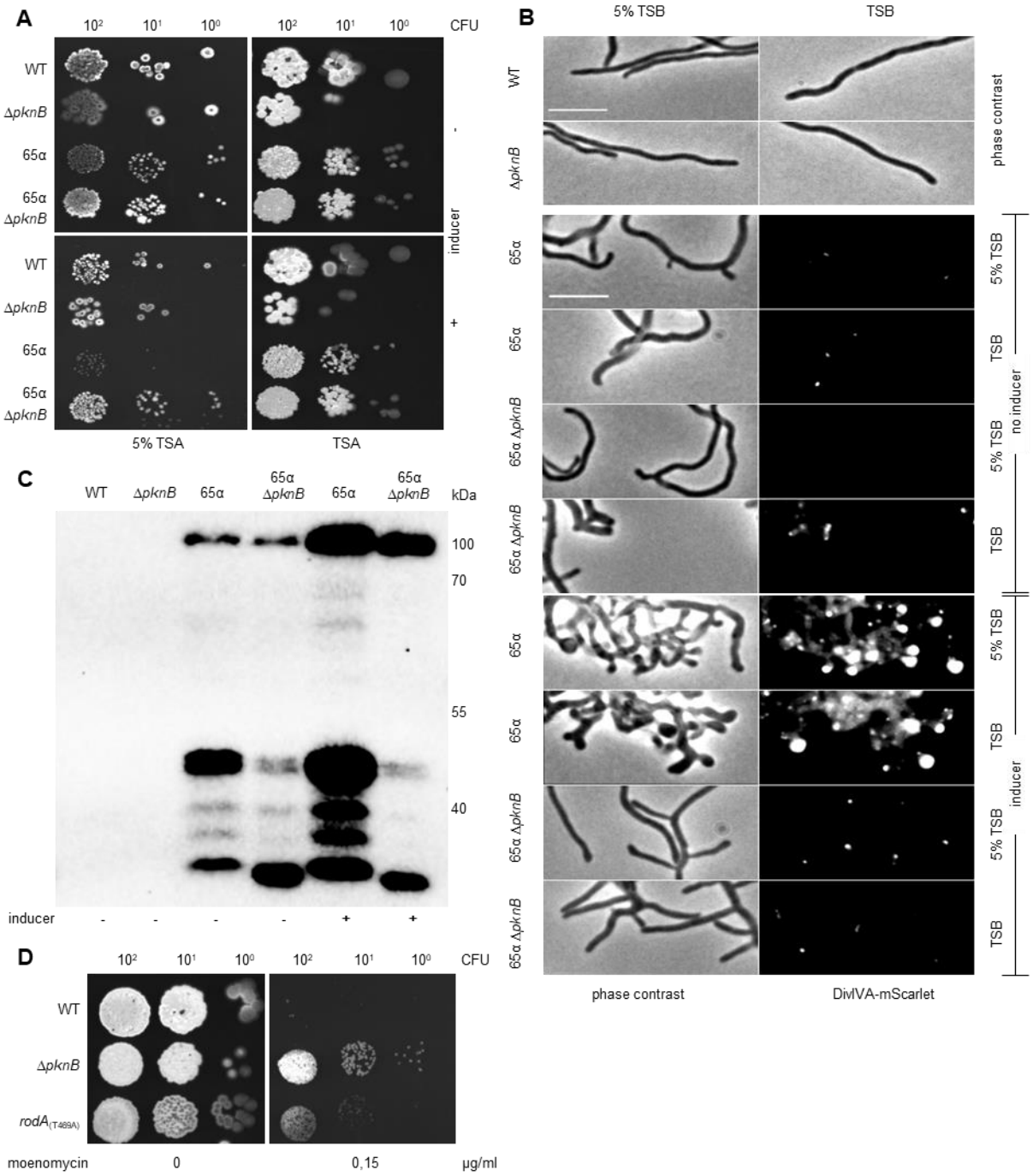

Figure 2 Verification of *pknB* deletion as suppressor of lethal DivIVA overproduction (A) Survival assay of *S. albus* J1074 strains grown on 5% TSA or TSA, in presence or absence of the inducer - ATc 500 ng/ml. (B) Phenotypes of *S. albus* J1074 strains grown in 5% TSB or TSB, in presence or absence of the inducer - ATc 250 ng/ml. Fluorescent microscopy shows DivIVA-mScarlet production. Scale bar - 5 µm. (C) Western blot analysis of DivIVA-mScarlet (theoretical mass ~68 kDa) production by *S. albus* J1074 strains grown in TSB, in presence or absence of the inducer - ATc 250 ng/ml. Detection performed with anti-mCherry polyclonal antiserum. MW values to the right indicate the positions of marker proteins. (D) Moenomycin sensitivity of *S. albus* J1074 strains grown on TSA medium.

PknB indirectly alters the phosphorylation state of CslA

The kinase PknB has been reported to be involved in a variety of processes (*e.g.* cell division, peptidoglycan synthesis, protein synthesis and stress response) (13, 29, 30). To better understand its role in *S. albus* we analysed the phosphoproteome of wild type and Δ*pknB S. albus* strains. The results identified 27 phosphorylated proteins, of which three were significantly hypophosphorylated in the *pknB* mutant, while one was significantly hyperphosphorylated (

Table 2 and File S2; for proteomics data see File S3). We did not detect RodA in this study, perhaps because of the low levels of the protein or a scarcity of unique peptides. Interestingly, the hyperphosphorylated protein was cellulose synthase-like protein CslA on residue T17 (15). This protein localizes at hyphal tips and is responsible for the production of a beta-glucan-containing polysaccharide that is thought to provide additional physical protection, which is needed due to the continuous remodelling of the growing cell wall (31). Loss of this polymer impairs morphological development and stability of the cell wall (31, 32). CslA forms a protein complex with a copper radical oxidase GlxA and it is a known interaction partner of DivIVA in *S. coelicolor* (31).

To evaluate the effect of phosphorylation on the function of CslA, we constructed a phosphoablative ($cslA_{(T17A)}$) strain, and a deletion mutant. Initially, we assessed the sensitivity of both mutant strains to moenomycin, as CslA contains a GTase domain, but no change in resistance was observed (Fig. S7). Previous studies have shown that deletion of *cslA* increases sensitivity to lysozyme (32). Consequently, we tested the $cslA_{(T17A)}$ and Δ*cslA* strains for lysozyme sensitivity, including the *pknB* deletion strain for comparison. While the latter behaved similarly to the wild type, both *cslA* mutants displayed hypersensitivity to lysozyme, suggesting that phosphorylation is important for the activity of CslA (Fig. 3A).

Next, we used a lectin dye to stain β-glucans (Fig. 3B) and found that the signal at the tips of hyphae was completely abolished in the *cslA* knockout strain, similar to previously reported data on a *cslA* deletion strain (31, 32). Consistent with data from the lysozyme sensitivity assay, the phosphoablative strain ($cslA_{(T17A)}$) behaved similarly to the deletion strain when stained for β-

glucans, indicating that phosphorylation is likely required for the β-glucan synthetic activity of CslA.

Given that CslA was found to be hyperphosphorylated in the absence of *pknB*, we tested the Δ*pknB* strain for lysozyme sensitivity and β-glucan distribution. We saw no significant resistance in the Δ*pknB* strain compared to the wild type.

Overall, these data indicate that phosphorylation plays an important role in β-glucan production, although any role for PknB in this is likely to be indirect.

Table 2 Significantly different proteins phosphorylation of *S. albus* J1074 WT and Δ*pknB* strains grown in TSB medium.

locus_tag	**protein name**	**phosphorylation in Δ*pknB* vs WT**
XNR_RS17030	FolK	Hypophosphorylated ↓
XNR_RS11880	GroL	Hypophosphorylated ↓
XNR_RS08650	CslA	Hyperphosphorylated ↑
XNR_RS14580	SppA	Hypophosphorylated ↓

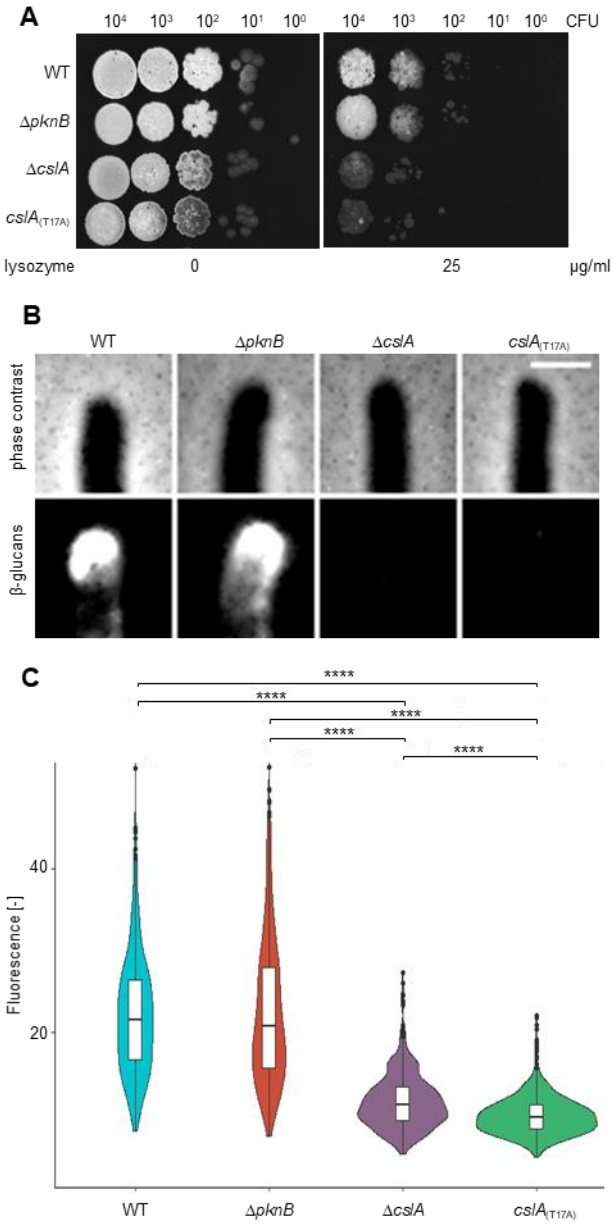

Figure 3 Assessment of β-glucan production by lysozyme sensitivity and single cell microscopy (A) Lysozyme sensitivity of *S. albus* J1074 strains grown on TSA. (B) Phenotypes of *S. albus* J1074 strains grown in TSB. Cells were stained with lectin dye to visualise β-glucans. An arrow points different β-glucans distribution along the hypha. Scale bar - 1 µm. (C) Mean β-glucans production at the tip by *S. albus* J1074 strains grown in TSB. The width of each plot indicates the amount of collected data points for specific fluorescence. Significant differences are marked with **** ($p \leq 0{,}0001$).

Summary and Conclusion

We aimed to identify proteins involved in modulating cell wall integrity and developed a new suppressor screen for this purpose. By overexpressing *divIVA* to lethal levels, we were able to select

and sequence spontaneously arising suppressor mutants, leading to the identification of the kinase PknB. A deletion of *pknB* in the *divIVA* overexpression mutant confirmed that PknB was indeed responsible for the lethality of the strain.

Next, we assessed the involvement of PknB in cell wall integrity and screened a *pknB* deletion mutant against various antibiotics. Notably, a PknB mutant displayed heightened resistance to the GTase-acting antibiotic moenomycin. While moenomycin targets the GTase activity of class A PBPs, it does not affect the RodA GTase (28). This suggests that the absence of PknB might increase RodA activity. To further investigate this process, we created a phosphoablative RodA mutant, which in turn made the strain hyper-resistant to moenomycin, confirming that PknB is phosphorylating RodA and that this is crucial for its activity (Fig. 4).

Since PknB was previously identified in a variety of processes, we conducted a global phosphoproteome to further understand the role of this kinase. Our results indicated that the cellulose synthase CslA is hyperphosphorylated in the absence of PknB. We then engineered both a deletion mutation of CslA and a phosphoablative strain. A mutation of residue T17 completely abolished the activity of CslA, identical to a deletion strain, as judged by quantitative microscopy and a lysozyme assay.

In conclusion, perturbing the cell wall synthetic machinery by overexpressing *divIVA* to lethal levels allowed us to identify PknB, and our findings demonstrate that PknB plays a crucial role in regulating cell wall integrity by phosphorylating RodA and CslA. This study enhances our understanding of how kinase PknB modulates cell wall integrity and suggests potential directions for future research into bacterial resistance mechanisms.

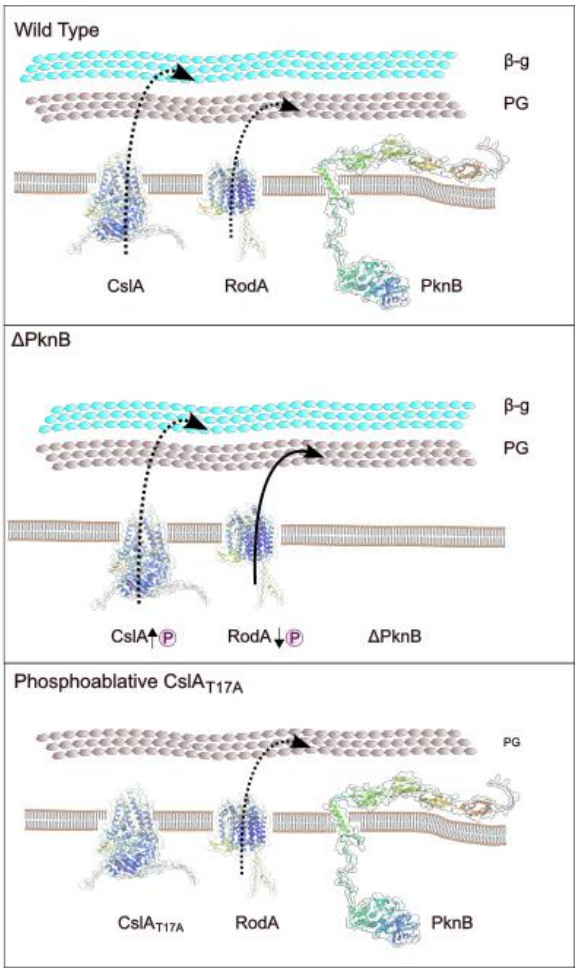

Figure 4 Proposed model of how phosphorylation regulates the cell wall stability in *Streptomyces* including the proposed roles of the kinase PknB and the cellulose like synthase CslA. Proteins structures were predicted by AlphaFold (33). Dotted line arrow indicates baseline activity of the enzyme. Full line arrow indicates increased activity of the enzyme. PG – peptidoglycan; β-g – β-glucans.

Author contributions

Conceptualisation (B.K., J.E.), Funding Acquisition (B.K., J.E.), Investigation (M.D., B.K, A.W., A.G.), Project administration (B.K.), Supervision (B.K., M.T., J.E.), Visualization (M.D., B.K.), Writing – original draft (M.D., B.K.,). writing – review and editing (M.D., B.K., D. J., J.E.)

Acknowledgements

This work was funded by the Polish National Science Centre: Sonata grant 2020/39/D/NZ1/00303 to B.K. and a Wellcome Trust Investigator grant (209500) to JE.

We further wish to express our gratitude to Dr Xiaobo Zhong (Leiden University) for useful discussion and advice regarding β-glucan staining.

Data availability

The genome sequencing data that support the findings of this study are openly available in NCBI at https://www.ncbi.nlm.nih.gov/sra (accession number PRJNA1099611).

The mass spectrometry proteomics data have been deposited to the ProteomeXchange Consortium via the PRIDE (34) partner repository with the dataset identifier PXD053764.

Reviewer access details:

Project accession: PXD053764

Token: tfcX8J5LlKQ2

References

1. Hempel AM, Wang SB, Letek M, Gil JA, Flärdh K. 2008. Assemblies of DivIVA mark sites for hyphal branching and can establish new zones of cell wall growth in Streptomyces coelicolor. J Bacteriol 190.

2. Flärdh K. 2003. Essential role of DivlVA in polar growth and morphogenesis in Streptomyces coelicolor A3(2). Mol Microbiol 49.

3. Richards DM, Hempel AM, Flärdh K, Buttner MJ, Howard M. 2012. Mechanistic Basis of Branch-Site Selection in Filamentous Bacteria. PLoS Comput Biol 8:e1002423.

4. Holmes NA, Walshaw J, Leggett RM, Thibessard A, Dalton KA, Gillespie MD, Hemmings AM, Gust B, Kelemen GH. 2013. Coiled-coil protein Scy is a key component of a multiprotein assembly controlling polarized growth in Streptomyces. Proc Natl Acad Sci U S A2013/01/09. 110:E397-406.

5. Fröjd MJ, Flärdh K. 2019. Apical assemblies of intermediate filament-like protein FilP are highly dynamic and affect polar growth determinant DivIVA in Streptomyces venezuelae. Mol Microbiol 112:47–61.

6. Elsholz AKW, Turgay K, Michalik S, Hessling B, Gronau K, Oertel D, Mäder U, Bernhardt J, Becher D, Hecker M. 2012. Global impact of protein arginine phosphorylation on the

physiology of Bacillus subtilis. Proceedings of the National Academy of Sciences 109:7451–7456.

7. Beilharz K, Nováková L, Fadda D, Branny P, Massidda O, Veening J-W. 2012. Control of cell division in Streptococcus pneumoniae by the conserved Ser/Thr protein kinase StkP. Proceedings of the National Academy of Sciences 109:E905–E913.

8. Kang CM, Abbott DW, Sang TP, Dascher CC, Cantley LC, Husson RN. 2005. The Mycobacterium tuberculosis serine/threonine kinases PknA and PknB: substrate identification and regulation of cell shape. Genes Dev 19:1692–1704.

9. Hempel AM, Cantlay S, Molle V, Wang SB, Naldrett MJ, Parker JL, Richards DM, Jung YG, Buttner MJ, Flärdh K. 2012. The Ser/Thr protein kinase AfsK regulates polar growth and hyphal branching in the filamentous bacteria Streptomyces. Proc Natl Acad Sci U S A 109.

10. Passot FM, Cantlay S, Flärdh K. 2022. Protein phosphatase SppA regulates apical growth and dephosphorylates cell polarity determinant DivIVA in Streptomyces coelicolor. Mol Microbiol 117.

11. Saalbach G, Hempel AM, Vigouroux M, Flärdh K, Buttner MJ, Naldrett MJ. 2013. Determination of phosphorylation sites in the DivIVA cytoskeletal protein of Streptomyces coelicolor by targeted LC-MS/MS. J Proteome Res 12.

12. Jani C, Eoh H, Lee JJ, Hamasha K, Sahana MB, Han JS, Nyayapathy S, Lee JY, Suh JW, Lee SH, Rehse SJ, Crick DC, Kang CM. 2010. Regulation of polar peptidoglycan biosynthesis by Wag31 phosphorylation in mycobacteria. BMC Microbiol 10.

13. Jones G, Del Sol R, Dudley E, Dyson P. 2011. Forkhead-associated proteins genetically linked to the serine/threonine kinase PknB regulate carbon flux towards antibiotic biosynthesis in Streptomyces coelicolor. Microb Biotechnol 4.

14. Arora D, Chawla Y, Malakar B, Singh A, Nandicoori VK. 2018. The transpeptidase PbpA and noncanonical transglycosylase RodA of Mycobacterium tuberculosis play important roles in regulating bacterial cell lengths. Journal of Biological Chemistry 293.

15. Henriques AO, Glaser P, Piggot PJ, Moran CP. 1998. Control of cell shape and elongation by the rodA gene in Bacillus subtilis. Mol Microbiol 28.

16. Lovering AL, Safadi SS, Strynadka NCJ. 2012. Structural perspective of peptidoglycan biosynthesis and assembly. Annu Rev Biochem https://doi.org/10.1146/annurev-biochem-061809-112742.

17. Mistry B V., Del Sol R, Wright C, Findlay K, Dyson P. 2008. FtsW is a dispensable cell division protein required for Z-ring stabilization during sporulation septation in Streptomyces coelicolor. J Bacteriol 190.

18. Kieser T, Bibb MJ, Buttner MJ, Chater KF. 2000. Practical Streptomyces Genetics. 2nd ed.International microbiology: official journal of the Spanish Society for Microbiology.

19. Watson AK, Kepplinger B, Bakhiet SM, Mhmoud NA, Chapman J, Allenby NE, Mickiewicz K, Goodfellow M, Fahal AH, Errington J. 2022. Systematic whole-genome sequencing reveals an unexpected diversity among actinomycetoma pathogens and provides insights into their antibacterial susceptibilities. PLoS Negl Trop Dis 16:e0010128.

20. Pospiech A, Neumann B. 1995. A versatile quick-prep of genomic DNA from gram-positive bacteria. Trends Genet 11:217–218.

21. Cingolani P, Patel VM, Coon M, Nguyen T, Land SJ, Ruden DM, Lu X. 2012. Using Drosophila melanogaster as a Model for Genotoxic Chemical Mutational Studies with a New Program, SnpSift. Front Genet 3.

22. Xiao W. 2015. Yeast Protocols 2nd EdMethods in molecular Biology.

23. Ehrlinger J, Blackstone EH. 2014. ggRandomForests : Survival with Random Forests. R Vignette 2.

24. Chawla Y, Upadhyay S, Khan S, Nagarajan SN, Forti F, Nandicoori VK. 2014. Protein kinase B (PknB) of Mycobacterium tuberculosis is essential for growth of the pathogen in vitro as well as for survival within the host. Journal of Biological Chemistry 289.

25. Fiuza M, Canova MJ, Zanella-Cléon I, Becchi M, Cozzone AJ, Mateos LM, Kremer L, Gil JA, Molle V. 2008. From the characterization of the four serine/threonine protein kinases (PknA/B/G/L) of Corynebacterium glutamicum toward the role of PknA and PknB in cell division. Journal of Biological Chemistry 283.

26. Matusiak I, Strzałka A, Wadach P, Gongerowska-Jac M, Szwajczak E, Szydłowska-Helbrych A, Kepplinger B, Pióro M, Jakimowicz D. 2023. The interplay between the polar growth determinant DivIVA, the segregation protein ParA, and their novel interaction partner PapM controls the Mycobacterium smegmatis cell cycle by modulation of DivIVA subcellular distribution . Microbiol Spectr 11.

27. Sieger B, Bramkamp M. 2015. Interaction sites of DivIVA and RodA from Corynebacterium glutamicum. Front Microbiol 5.

28. Emami K, Guyet A, Kawai Y, Devi J, Wu LJ, Allenby N, Daniel RA, Errington J. 2017. RodA as the missing glycosyltransferase in Bacillus subtilis and antibiotic discovery for the peptidoglycan polymerase pathway. Nat Microbiol 2.

29. Richard-Greenblatt M, Av-Gay Y. 2017. Epigenetic Phosphorylation Control of Mycobacterium tuberculosis Infection and Persistence . Microbiol Spectr 5.

30. Dworkin J. 2015. Ser/Thr phosphorylation as a regulatory mechanism in bacteria. Curr Opin Microbiol 24:47.

31. Xu H, Chater KF, Deng Z, Tao M. 2008. A cellulose synthase-like protein involved in hyphal tip growth and morphological differentiation in streptomyces. J Bacteriol 190.

32. Zhong X, Zhang L, van Wezel GP, Vijgenboom E, Claessen D. 2022. Role for a Lytic Polysaccharide Monooxygenase in Cell Wall Remodeling in Streptomyces coelicolor. mBio 13.

33. Jumper J, Evans R, Pritzel A, Green T, Figurnov M, Ronneberger O, Tunyasuvunakool K, Bates R, Žídek A, Potapenko A, Bridgland A, Meyer C, Kohl SAA, Ballard AJ, Cowie A, Romera-Paredes B, Nikolov S, Jain R, Adler J, Back T, Petersen S, Reiman D, Clancy E, Zielinski M, Steinegger M, Pacholska M, Berghammer T, Bodenstein S, Silver D, Vinyals O, Senior AW, Kavukcuoglu K, Kohli P, Hassabis D. 2021. Highly accurate protein structure prediction with AlphaFold. Nature 596.

34. Perez-Riverol Y, Bai J, Bandla C, García-Seisdedos D, Hewapathirana S, Kamatchinathan S, Kundu DJ, Prakash A, Frericks-Zipper A, Eisenacher M, Walzer M, Wang S, Brazma A, Vizcaíno JA. 2022. The PRIDE database resources in 2022: A hub for mass spectrometry-based proteomics evidences. Nucleic Acids Res 50.